

Structural Configuration and Building Energy Performance

Mohamed Krem¹; Simi T. Hoque²; Sanjay R. Arwade³; and Sergio F. Breña, M.ASCE⁴

Abstract: The civil engineering and architectural communities are highly focused these days on designing buildings that maximize utilization of energy available from natural resources through means such as passive solar heating and passive ventilation and minimizing the consumption of energy produced external to the building itself. Indeed, so-called net-zero-energy buildings, which would require no net energy input for their operation, have been identified as an aspirational goal for architects and engineers. It has been suggested that for each of the four major climate zones there exists an optimal building morphology, consisting of floor plan geometry and placement of the primary structural system for lateral loads, the structural core or wall, which contains major mechanical services and vertical transportation conduits. This paper presents a quantitative study of the effect of building morphology on energy performance in each of the four climate zones. The energy analysis is performed using Autodesk Ecotect Analysis 2011. Four building morphologies are investigated, each representing a high-rise commercial building with equivalent area, height, and material use. For comparison, results are presented in terms of annual sensible heating and cooling loads. A three-dimensional rendering of how the different building types might respond under wind loads is presented to indicate how the environmental and structural performances become coupled when the building is designed only with environmental performance in mind. DOI: [10.1061/\(ASCE\)AE.1943-5568.0000103](https://doi.org/10.1061/(ASCE)AE.1943-5568.0000103). © 2013 American Society of Civil Engineers.

CE Database subject headings: Sustainable development; Energy efficiency; Building design; Solar power.

Author keywords: Efficiency; Comfort; Passive solar; Skyscraper; Morphology; Sustainable.

Introduction

Improving the energy efficiency of medium- to high-rise buildings is a key component in increasing the sustainability of the built environment. More than one-third of the world's energy consumption is attributed to the construction and building industry (Straube 2006). Given the current state of global energy demand, there is a critical need to design and construct buildings that are more sustainable. Sustainable buildings minimize building resource consumption, operations and life-cycle costs, and improve occupant health and comfort (Straube 2006).

Substantial progress has been made toward improved energy efficiency through design and technological innovations such as passive ventilation systems, day lighting and sun shading, high performance heating, cooling, and ventilation (HVAC) systems, and the introduction of novel materials to the building envelope. However, the impact and influence of the structural system on building energy efficiency has been largely neglected as a research and design issue; therefore, it serves as the focus of this paper. Whether structural and energy performance considerations can be integrated and optimized concurrently is considered. Tradeoffs in the design of

structural systems for both structural and energy performance are also analyzed.

This analysis is predicated on the proposition that the structural system of a building can be optimized to improve energy efficiency in addition to resisting gravity and lateral loads. In his book *The Green Skyscraper* (Yeang 1999), architect Kenneth Yeang suggests that in different climate zones the structural core/wall should be arranged in different configurations to reduce the yearly energy consumption of the building. Furthermore, he argues that the shape of the building footprint should be modified based on the climate zone in which the building is to be constructed (Fig. 1). In Yeang's analysis, three parameters are varied: (1) the shape of the building floor plan, (2) the placement of the structural core or cores, and (3) the orientation of the building floor plan. The first two of these parameters have clear implications on structural performance because buildings with asymmetric distribution of stiffness are known to be susceptible to damaging torsional modes of vibration when subjected to wind or earthquake loading. However, Yeang does not address the implications of different floor plans and core/wall placement on structural performance. As for the third parameter, building orientation has much less effect on structural performance unless the building is located where wind direction is strongly biased.

In the current study, Yeang's proposals inspire an examination of the design of the structural system of high-rise buildings for energy efficiency and structural performance. Because the design space for tall building structural systems is extremely large, Yeang's proposed building types are used to define a reduced design space that nevertheless covers many possible configurations of structural system. It is considered how two parameters (the shape of the building floor plan and the placement of the structural cores), which are called the building morphology, influence energy performance. Although material choice can potentially have significant effects on environmental and structural performance, this variable is maintained as constant to focus on the relationship between building morphology and energy efficiency.

¹Ph.D. Candidate, Dept. of Civil and Environmental Engineering, Univ. of Massachusetts, Amherst, MA 01003.

²Assistant Professor, Dept. of Environmental Conservation, Univ. of Massachusetts, Amherst, MA 01003.

³Associate Professor, Dept. of Civil and Environmental Engineering, Univ. of Massachusetts, Amherst, MA 01003 (corresponding author). E-mail: arwade@ecs.umass.edu

⁴Associate Professor, Dept. of Civil and Environmental Engineering, Univ. of Massachusetts, Amherst, MA 01003.

Note. This manuscript was submitted on October 18, 2011; approved on July 10, 2012; published online on February 15, 2013. Discussion period open until August 1, 2013; separate discussions must be submitted for individual papers. This paper is part of the *Journal of Architectural Engineering*, Vol. 19, No. 1, March 1, 2013. ©ASCE, ISSN 1076-0431/2013/1-29-40/\$25.00.

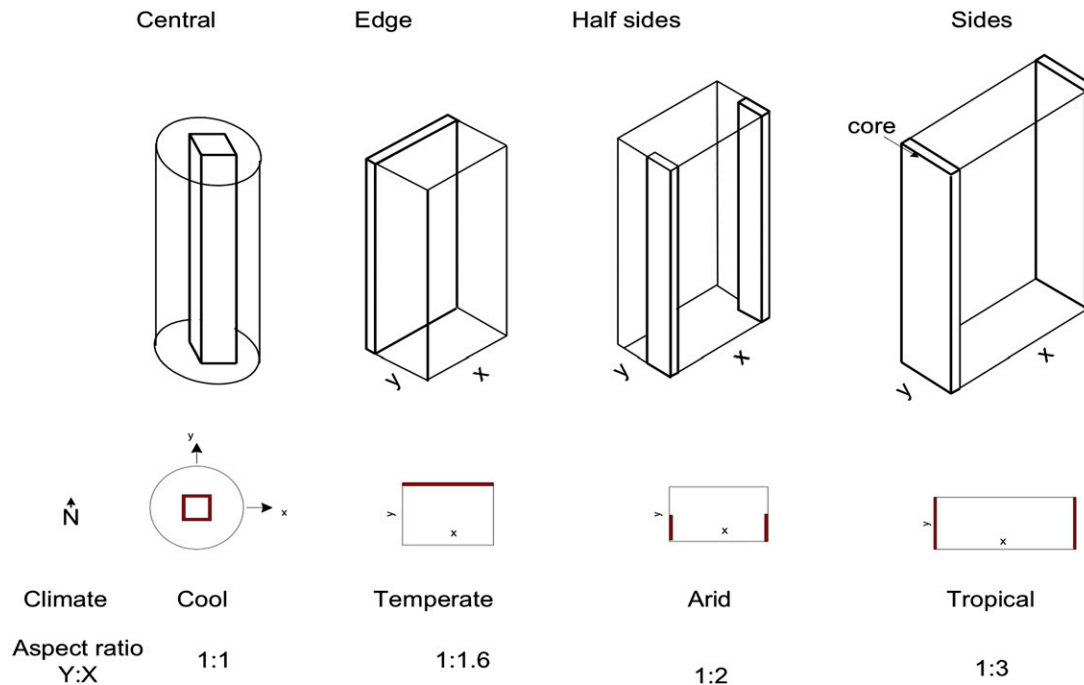


Fig. 1. Proposal by K. Yeang for optimal floorplan and placement of structural cores to minimize building energy consumption in four climate zones (adapted from Yeang 1999)

Previous studies have shown that solar heat gain plays a major role in driving the energy demand to maintain comfort in buildings. Jones et al. (1982) studied, in varying climates, passive solar design, energy conservation strategies, and the harvesting of solar energy to save in the cost of annual energy demand. Furthermore, they developed a method for determining the optimal mix of energy conservation strategies and solar energy harvesting, emphasizing that the designer should always consider the “trade-off between the cost of the improvement versus the increased performance.” They recommended that energy conservation should be emphasized over solar energy harvesting where cooling is the major demand and recommended shading tactics be implemented to prevent the features of passive solar heating from unduly increasing cooling loads in the summer.

Mazria (1979) provided a complete guide to passive solar home, greenhouse, and building design, which illustrates many different applications of direct heat gain concepts for both commercial and residential buildings. In terms of building shape, he recommended, for all climates, that the optimal building is elongated in an east-west direction, resulting in more exposed surface area facing south. This configuration minimizes heating needed in winter and cooling in summer. Also, he emphasized that in climates where heating is needed in winter, the building should be positioned on the site that receives the most sun during the hours of maximum solar radiation from 9 a.m. to 3 p.m. “to insure that the outdoor areas and gardens placed to the south will have adequate winter sun, and help minimize the possibility of shading the building in the future by off-site developments.”

Other studies have shown the potential for structure to play a positive role in influencing the energy performance of buildings. For example, Chow (2004) showed that a structural wall projecting from the building façade could guide prevailing winds to drive passive ventilation of a tall building. Mak et al. (2007) investigated the effect of wing walls on passive ventilation and found potential synergies between the structure and environmental performance. Li and Mak (2007) used simulations to evaluate the performance of a wind catcher device designed for passive ventilation.

Additionally, the structural engineering profession has been attempting to define the proper role for the structural engineer in the pursuit of sustainability of the built environment. Anderson and Silman (2009) and Webster (2004) identified the role of the structural engineer in an integrated design team of architects, engineers, builders, and owners to make the structure sustainable. The Structural Engineering Institute of the ASCE has recently published *Sustainability Guidelines for the Structural Engineer* (Kestner et al. 2010), which provides guidance on how to reduce environmental impacts for all common material types. These publications promise to significantly affect the way that structural engineering is practiced, yet none of them directly address the interplay of structural form and energy efficiency, which is the primary interest in this paper.

In the following sections, the problem is defined to evaluate the energy and structural performance of four different building morphologies in four different climate zones. The results of structural and energy consumption calculations are then presented for each of the 16 morphology/climate scenarios, and finally, the results are discussed, and conclusions are presented.

Problem Statement

Two characteristics of the building morphology are considered in this study as design variables that can be modulated to optimize high rise thermal performance: the position of the vertical structural core/wall and the aspect ratio and shape of the floor plan (Fig. 1). All other morphological descriptors such as the square footage, number of stories, building height, occupancies, and envelope materials for the four skyscraper office buildings are constant. All are 200 m in height, with 50 stories that are 4.0 m floor-to-floor height, with a total conditioned floor area of 135,000 m². Because of the complex nature of the interactions between the building envelope and structural system, it is impossible to design numerical experiments with truly

controlled variables. For example, and particularly relevant to this study, changing the structural core configuration changes the percentage of the building envelope that is glazed.

Fig. 2 shows the plan views for these models and the locations of the primary mass (opaque surfaces) and the glazing walls (transparent surfaces) for each configuration. The primary material for the structural core/wall (opaque walls) is reinforced normal weight concrete, and the glazed (curtain) walls are layers of standard glass and 10% metal framing. To simplify the analysis of the energy consumption, the effect of surrounding buildings and of building orientation is neglected, in essence assuming that the buildings are erected on flat open ground and are aligned with the cardinal

directions. The structural content of the core/wall is admittedly simple—normal RC shear walls—yet this system captures the two important contributions of the structural core/wall to environmental performance: opacity of the building envelope leading to shading of the interior and thermal mass. Because the shear walls are assumed to be of the same material and thickness in each of the four morphologies, this simplified structural system can also give reasonable estimates of the stiffness distribution in the building. As previously mentioned, the percentage glazed area is not constant over the four building types, and the percentage of glazed area, in and of itself, can have a significant effect on energy performance. One could achieve constant glazed area across the four building types by modifying the

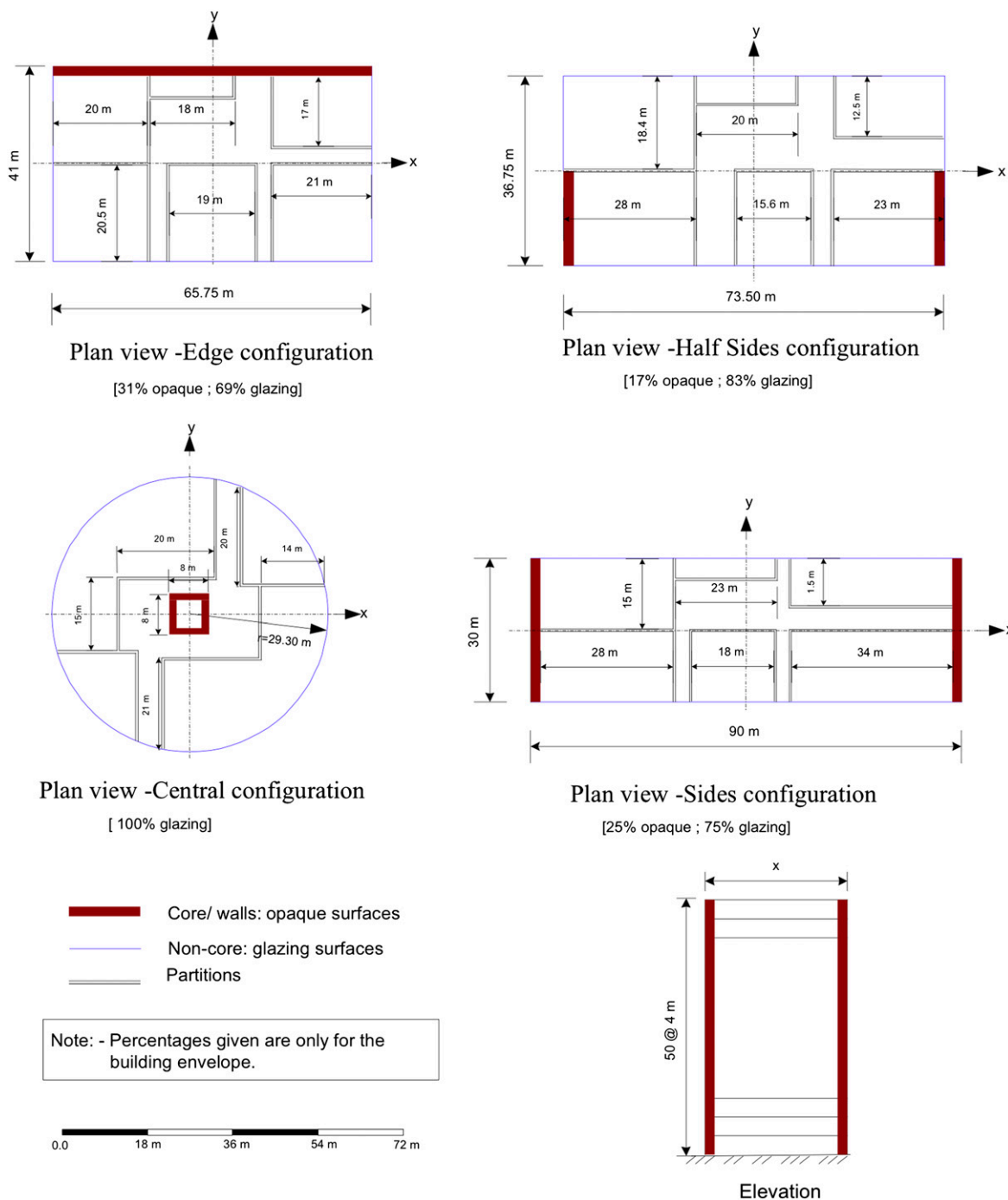


Fig. 2. Plan views and an elevation of the buildings

Table 1. Description of the Climate Zones Characteristics for the Representative Cities

Characteristics	Boston (cool zone)	Sacramento (temperate zone)	Las Vegas (arid zone)	Honolulu (tropical zone)
Average temperatures (°C)				
High	23.3	24–32	34–40	27–32
Low	–1.5	7.7–16	21–26	19–24
Dry bulb temperature (°C)				
Maximum	37.2 (on Jul. 9)	42.0 (on Jun. 14)	44.4 (on Jul. 4)	33.3 (on Sep. 2)
Minimum	–20.0 (on Jan. 23)	–2.0 (on Feb. 2)	–3.3 (on Feb. 16)	13.3 (on Feb. 12)
Annual degree-days (18°C baseline)				
Cooling	490	670	1,904	2,524
Heating	3,120	1,436	1,234	0.0
Average daytime	11 h, 45 min	12 h, 24 min	11 h, 15 min	12 h
Average nighttime	12 h, 15 min	11 h, 36 min	12 h, 45 min	12 h
Average annual rainfall (mm)	1,080 and 1,060 of snowfall	545	110	460
Maximum wind speed (m/s)	21.6 (on Sep. 6)	17.0 (on Mar. 4)	20.6 (on Apr. 12)	13.4 (on Nov. 15)

properties of the architectural envelope, and this issue has been addressed elsewhere (Krem 2012).

All four building morphologies are simulated in each of the four major climate zones [cool, temperate, arid, and tropical, according to the Koppen classification (Kottek et al. 2006)]. Additionally, specific cities have been selected as representative of the conditions in each climate zone, and the climatic conditions at these four sites were used in the building energy performance simulations: Boston, for the cool zone; Sacramento, California, for the temperate zone; Las Vegas for the arid zone; and Honolulu, Hawaii, for the tropical zone. The climate characteristics for the representative cities are provided in Table 1 (U.S. Department of Energy 2010).

Building energy consumption is highly dependent on the occupancy and use of the interior space. Because the goal is to isolate the influence of building morphology on energy consumption, occupancy and use characteristics are assumed to be constant across all climate zones and building types. Specifically, the thermostat range, internal design conditions, occupancy, infiltration rate, and hours of operation are treated as fixed control parameters, set at reasonable values for an office building (Table 2) [American Society of Heating, Refrigerating and Air-Conditioning Engineers (ASHRAE) 2010; Chartered Institution of Building Services Engineers (CIBSE) 2006].

The materials selected for the exterior envelope of all four models meet the requirements of thermal resistance of the 2009 International Energy Conservation Code (IECC) (U.S. Department of Energy Building Energy Codes Program 2010) for its specific climate zone. Accordingly, there are three different material palettes (with associated thermal resistances) for the four buildings. In other words, there is a prescribed material palette for the buildings in the Tropical Zone 1, for buildings in the temperate zone and arid zone (both Zone 3), and for buildings in Cool Zone 5. Structural layers and thermal resistance of the material are presented in Table 3.

Thermal Analysis (Energy Performance)

For the remainder of this paper, the following naming convention will be used for the proposed configurations depending on where the structural cores/wall are placed in the buildings (opaque walls): central for cool zone; edge for temperate zone; half sides for the arid zone; sides for the tropical zone.

Energy Modeling

Autodesk's *Ecotect* energy simulation package (Autodesk Education Community 2011) was used for the thermal analysis. *Ecotect 2011* is

Table 2. Thermal Analysis Conditions (Values from ASHRAE 2010 and CIBSE 2006)

Parameters	Values
Active system	Full air conditioning
Thermostat range (°C)	18–26
Occupancy (people) (m ² /person)	12
Occupancy (activity) (W/person)	70
Internal design conditions (clothing) (clothing/person)	1
Internal design conditions (relative humidity) (%)	60
Internal design conditions (air speed) (m/s)	0.5
Internal design conditions (lighting level) (lx)	300
Infiltration (air change rate) (/h)	0.5
Internal heat gain (W/m ²)	10
Hours of operation	Schedule

a comprehensive concept-to-detail sustainable building design program; it is a popular program used by architects, as its modeling procedure is simple, it is easy to rapidly manipulate the properties of models, and it consumes a reasonably short run time for large models. The *Ecotect* procedure starts with creating a three-dimensional (3D) shell that represents the building form. This can be done in one of two ways: (1) draw plans representing the boundary of the rooms, continuing room by room to form a 3D model, or (2) import the model as a gbXML file from a different 3D modeling program such as Revit. For this analysis, the building's geometry was prepared in *Revit 2010* (Autodesk Education Community 2011), and the 3D model as surfaces and rooms was imported to *Ecotect 2011*. After the import, thermal properties are assigned to the building's envelope and the analysis proceeds. The basic material of an element (concrete wall, slab, glazing wall, etc.) is assigned first, and then the resistance (*R* value) of the insulation is applied according to the specifications of the IECC code as presented in Table 3. The next step is to assign a weather file that corresponds to the climatic zones selected for this study and to provide occupancy and scheduled use data. Finally, the program can calculate monthly and annual heating and cooling loads according to given climate conditions.

Modeling Assumptions

For the purpose of this study, several assumptions are made: (1) all the buildings have equivalent square footage, height, material use,

Table 3. Structural Materials and Thermal Resistance of the Building Components (U.S. Department of Energy Building Energy Codes Program 2010)

Building element	Zone 1 (tropical)			Zone 3 (arid and temperate)			Zone 5 (cool)		
	Materials	Resistance		Materials	Resistance		Materials	Resistance	
		U W/m ² K	R m ² K/W		U W/m ² K	R m ² K/W		U W/m ² K	R m ² K/W
Core/wall	450 mm normal concrete	1.65	0.61	450 mm normal concrete, 22 mm polyfoam, 10 mm plaster in either side	0.74	1.36	450 mm normal concrete, 45 mm polyfoam, 10 mm plaster in either side	0.49	2.05
Glazing walls	6 mm single glazed metal framing	6.81	0.15	6 mm double glazed metal framing, 16 mm gap with low-conductance gas fill	3.40	0.294	6 mm double glazed metal framing, 13 mm gap with low-conductance gas fill	9.3	0.107
Roof	27 mm aggregate, 6 mm asphalt, 100 mm normal concrete, 19 mm polyfoam, 10 mm plaster	0.37	2.71	27 mm aggregate, 6 mm asphalt, 100 mm normal concrete, 27 mm polyfoam, 10 mm plaster	0.267	3.75	27 mm aggregate, 6 mm asphalt, 100 mm normal concrete III, 27 mm polyfoam, 10 mm plaster	0.267	3.75
Suspended floor	10 mm ceramic tiles, 5 mm screed, 100 mm concrete floor, 50 mm air gap, 10 mm plaster underneath	1.81	0.55	10 mm ceramic tiles, 5 mm screed, 100 mm suspended concrete floor, 20 mm polystyrene, 50 mm air gap, 10 mm plaster underneath	0.86	1.17	10 mm ceramic tiles, 5 mm screed, 100 mm suspended concrete floor, 40 mm polystyrene, 50 mm air gap, 10 mm plaster underneath	0.27	3.75
Slab on ground	100 mm concrete, 5 mm screed, 10 mm ceramic tiles	0.88	1.14	100 mm concrete, 5 mm screed, 10 mm ceramic tiles	0.88	1.14	100 mm concrete, 5 mm screed, 10 mm ceramic tiles	0.88	1.14
Partition	80 mm framed wall as air gap, 10 mm plaster board either side	2.21	0.45	80 mm framed wall as air gap, 10 mm plaster board either side	2.21	0.45	80 mm framed wall as air gap, 10 mm plaster board either side	0.21	0.45

and thermal properties; (2) all the buildings are oriented orthogonal with the cardinal directions (Fig. 2); and (3) to simplify the analysis, because one cannot define curved building boundaries in *Ecotect*, the circular shape of the central configuration has been replaced by a dodecagon (12-sided) shape with equivalent floor area.

Analysis

The thermal analysis involves examining each of the four models (central, edge, half sides, and sides) in each of the four climatic zones (cool, temperate, arid, and tropical). This constitutes 16 different simulation runs, each of which requires approximately 24 h to complete. For each climate zone, weather data (TMY files) for each city are loaded, and the four models are tested under equal thermal conditions. That is, the only differences among the four runs in the same climate zone are the floor plan shape and the placements of the structural core/walls. This analysis considers only sensible heating and cooling loads and neglects hygrothermal effects of moisture sorption/desorption in building materials.

Ecotect calculates the effect of solar insolation on the heating/cooling loads of each building. Different climate zones have different effects; for example, in the tropical zone, the heating demand is negligible (effectively zero) throughout the year (Table 4), and cooling loads dominate. It would follow, therefore, that to reduce

cooling loads in the tropical zone, direct heat gain as a result of solar insolation must be minimized. In this case Yeang suggests using the core to shade the building on the east and west sides (sides configuration). Fig. 3 shows the sun-path diagram and how the building is shaded by its side walls (location at 12:15 p.m., Aug. 20, Honolulu, Hawaii). Table 4 indicates that the sides model—elongated in the east-west (EW) direction—is optimal in all four climate zones. The finding that an EW-elongated form is optimal for energy performance even in hot climates is somewhat unconventional but is supported by the work of Mazria (1979).

Thermal Analysis Results

The thermal analysis results are presented in two sections. The first section demonstrates the results graphically in four figures (Figs. 4–7). Each figure represents the monthly cooling and heating loads for each of the four configurations per climatic zone. The second section presents tabulated values of annual energy use for heating and cooling loads, energy use intensity, and the difference between Yeang's recommended configuration and the configuration that resulted in the lowest energy consumption.

Fig. 4 shows the result of the thermal analysis of the four models in an arid climate (Las Vegas). Generally, for all configurations, the heating load is highest during the winter months (December and

Table 4. Annual Heating and Cooling Loads

Item measured	Central		Edge		Half sides		Sides		Yeang recommendation	% diff.
	Heating (Mwh)	Cooling (Mwh)								
Zone: Cool										
Loads	7,538	875	5,992	877	6,553	816	5,548	777	Central	32
Σ	8,414		6,869		7,369		6,326			
%	89.59	10.41	87.23	12.76	88.93	11.1	87.71	12.29		
EUI (kwh/m ²)	62.3		51		54.6		46.86			
Zone: Temperate										
Load	1,310	3,646	946	3,443	1,103	3,476	884	3,248	Edge	6.5
Σ	4,956		4,389		4,578		4,132			
%	26.4	73.6	21.6	78.4	24.1	75.9	21.4	78.6		
EUI (kwh/m ²)	36.7		32.5		33.92		30.61			
Zone: Arid										
Load	990	7,647	696	6,904	841	7,167	673	6,677	Half sides	8.0
Σ	8,637		7,600		8,009		7,350			
%	11.5	88.5	9.2	90.8	10.5	89.5	9.16	90.8		
EUI (kwh/m ²)	63.9		56.3		59.32		54.44			
Zone: Tropical										
Load	0.0	7,824	0.0	7,612	0.0	7,746	0.0	7,372	Sides	0
Σ	7,824		7,612		7,746		7,372			
%	0.0	100	0.0	100	0.0	100	0.0	100		
EUI (kwh/m ²)	57.9		56.4		57.4		54.61			

Note: % diff = percentage of a load (heating or cooling) from the total load [the summation (Σ) of heating and cooling].

January). The heating demand decreases gradually thereafter until April, when the building switches to cooling mode. The maximum cooling demand occurs during the months of July and August. For this climate, the annual demand for cooling is significantly higher (approximately seven times) than heating, which is reasonable for a desert climate. Notably, the central configuration building has the highest cooling load compared with the other models. The sides configuration demands the least energy, whereas the edge model has the second lowest cooling load rank and the half sides is ranked third.

Fig. 5 presents the thermal analysis results for a cool climate zone (Boston). In general, the loads are dominated by heating demand for most of the year, which is typical for this climate. For the cooling load, confined mostly to the month of August, the comparative differences among all four models are small. The demand of annual total energy is the lowest in the sides model, the central model has the highest energy profile, and the other two models (edge, half sides) are ranked second and third, respectively.

Fig. 6 illustrates the thermal analysis in a temperate climate (Sacramento, California). Monthly energy load simulates the seasonal changes in temperature, precipitation, and solar insolation. Moreover, in a temperate climate, the need for energy is greatest for 7 months of the year. Four months (June through September) are dominated by cooling loads, which are approximately twice what is required for heating during the other 3 months (December through February). The results demonstrate that the annual energy consumption is the lowest in the sides model. The edge model is ranked

second (which was recommended by Yeang for this climate), and the half sides and central models are ranked third and fourth, respectively.

Fig. 7 presents the thermal analysis for a tropical climate (Honolulu, Hawaii). In this climate, the total energy demand is for cooling. In addition, the energy demand is highest in the summer and is greatly reduced during the winter season. Throughout the year, cooling is required. The model with the lowest energy profile is the sides configuration, which was recommended by Yeang. This model maintains comfort with the lowest energy consumption, whereas edge, half sides, and central models rank second, third, and fourth, respectively.

In general, these plots show how monthly energy loads fluctuate between cooling and heating corresponding to the seasonal climate. Although the interest is in total yearly energy use, it can be instructive to examine monthly use statistics. For example, Fig. 4 shows that the ordering of the consumption associated with the four morphologies is consistent throughout the year in the arid climate, but in Figs. 6 and 7, the ordering changes from month to month. Such monthly variations would be considered as architectural treatments such as shading devices are designed to improve energy performance. Another interesting observation from the figures is that the ordering of energy consumption among the morphologies is not always consistent for heating and cooling loads. For example, Fig. 5 shows that the side configuration uses the least energy for heating and cooling but that the second most efficient morphology is edge for heating and half sides for cooling. Such a seasonal analysis is

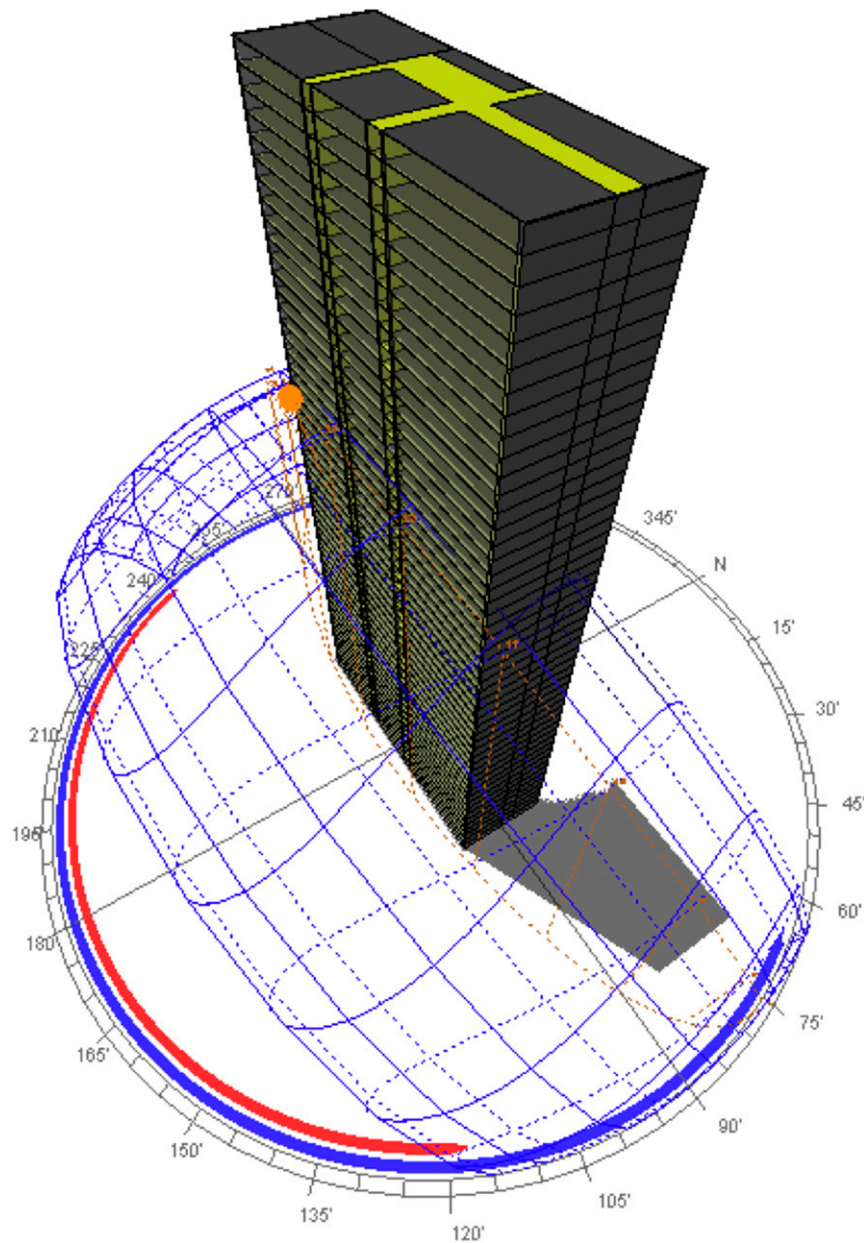


Fig. 3. Sun-path diagram of sides model in tropical zone illustrating building wall shadow

important because different energy sources are typically used for heating and cooling, and the costs and carbon emissions associated with each source may differ substantially.

The annual energy loads are presented in Table 4. Each row represents the results of examining each model configuration (central, edge, half sides, and sides) in a single climatic zone. The first row illustrates the thermal results in a cool climate. The annual loads for this climate are dominated by heating demand. This is an indication that the heating load should be viewed as a priority in optimizing energy efficiency rather than total heating and cooling demand. In this analysis, the sides model represented the lowest energy use intensity (EUI) and heating demand. Yeang's recommended configuration is the central model. The use of the sides model in a cool climate might result in a 32% reduction in energy consumption, 16% in the case of use of the half sides model, and 9.6% in the case of use of the edge model compared with the recommended configuration (central). These differences are

significant. The lowest ranking configuration—with the highest energy penalty—is Yeang's central model.

The second row lists results for each configuration in a temperate climate. According to the data from the weather file, this climate is dominated by cooling degree-days, which represents 68% of energy demand (Table 1). This is consistent with the results obtained from thermal analysis, where the cooling load averaged 76.6% for all four building configurations. The model that consumes the least amount of cooling energy is likely the most appropriate configuration for this climate. This is true of the sides model, which has the lowest cooling load by a factor of 6.0% compared with Yeang's recommended configuration (edge). Also, this is very close to the percentage difference in annual total energy demand between these two models. The edge model is the second ranking configuration, although the cooling load in the half sides model only differs by 1% compared with the edge model (recommended configuration). The least favorable configuration is the central model. The total energy demand

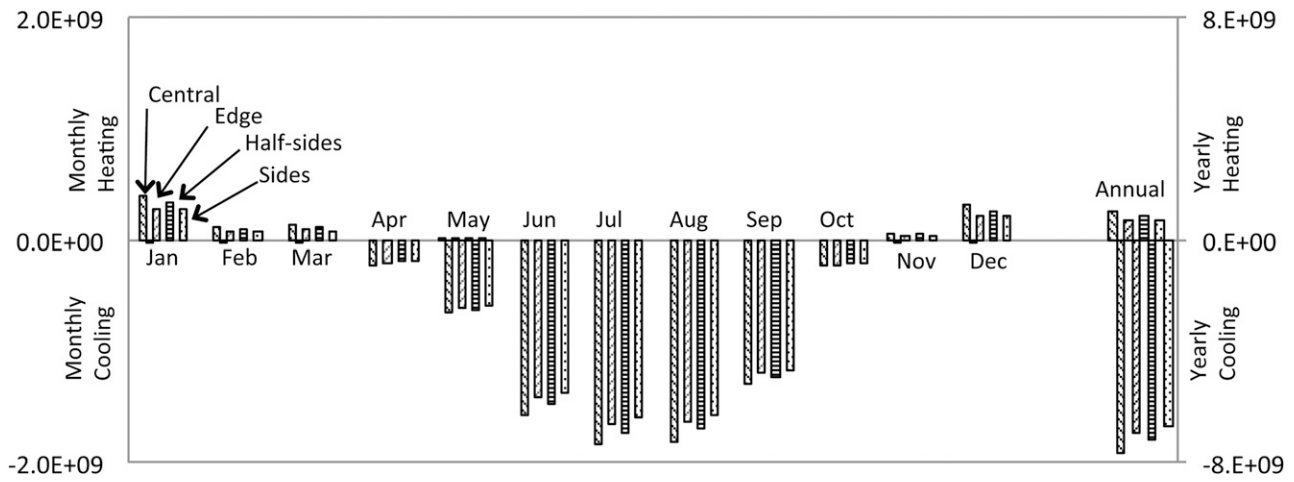


Fig. 4. Thermal analyses results of the four models in arid climate

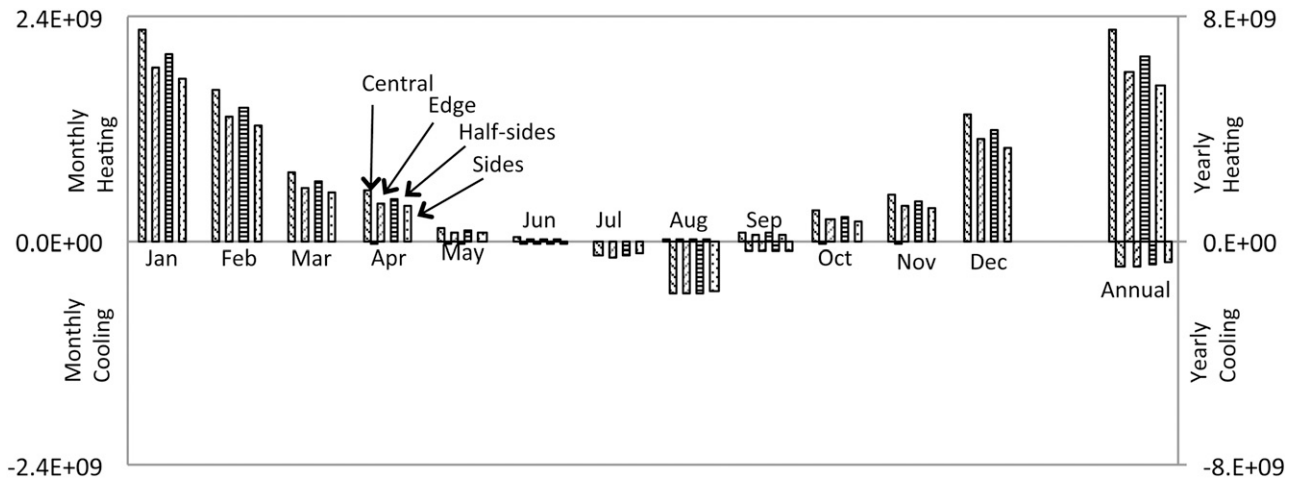


Fig. 5. Thermal analyses results of the four models in cool climate

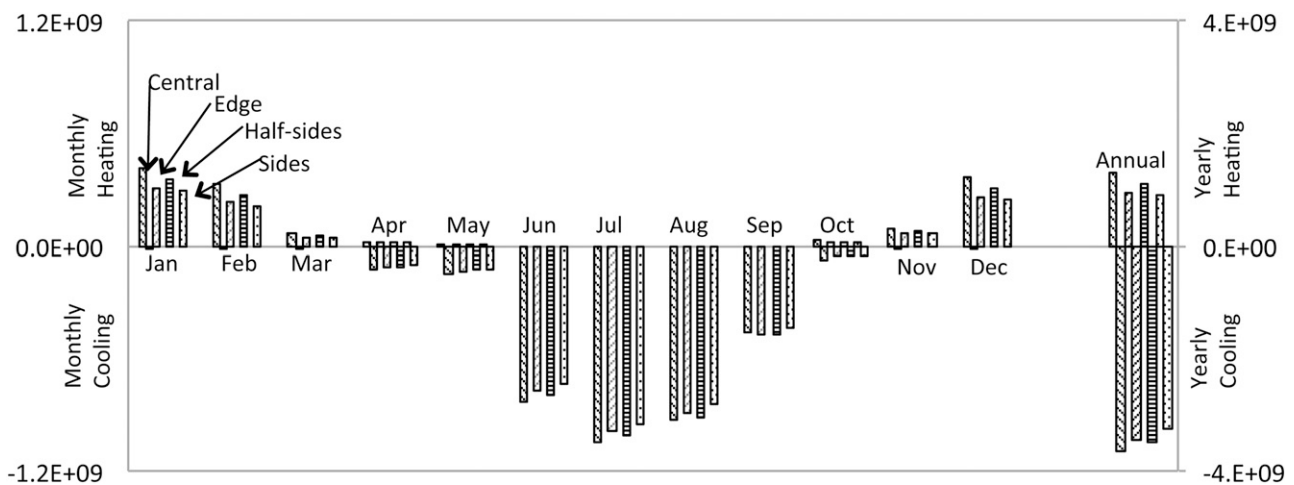


Fig. 6. Thermal analyses results of the four models in temperate climate

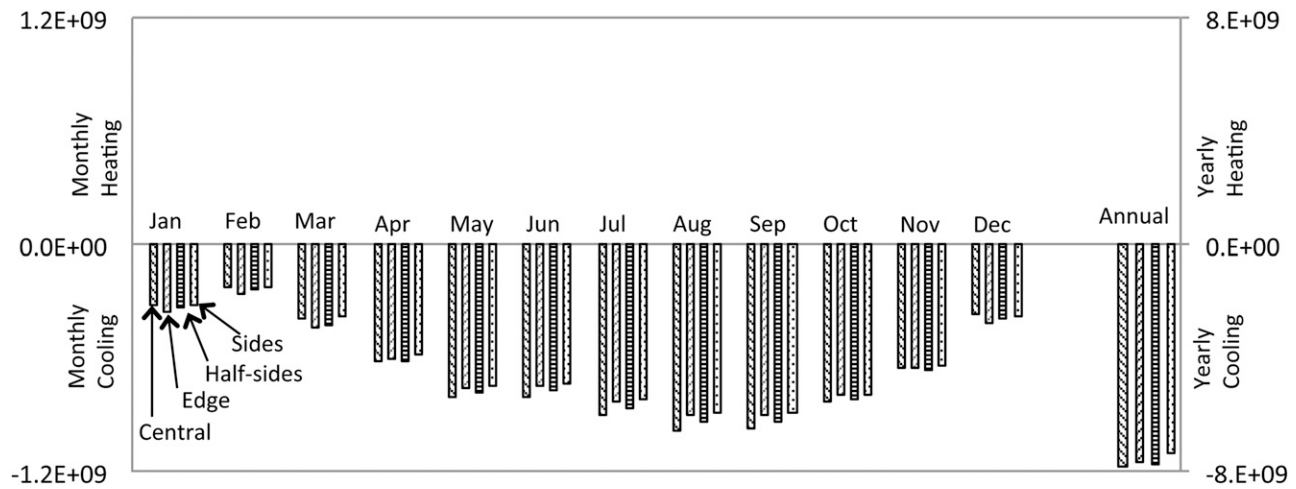


Fig. 7. Thermal analyses results of the four models in tropical climate

of the central model exceeds the sides model by 20%, 13% for the edge model, and 8% for the half sides model.

The third row represents the thermal analysis results for an arid climate. The average breakdown cooling and heating loads are 91.6% for cooling and 8.4% for heating. Nevertheless, in all cases, the cooling load is the higher percentage of the total energy need in this climate. The cooling energy demand is the lowest in the sides model, with a difference of 7% compared with Yeang's recommendation (half sides), which ranked third. The difference in EUI is 3.7% between the edge model (second option) and the half sides model (recommended model). The least favorable configuration for this climate is the central model with higher energy consumption, exceeding the annual load for the sides configuration by 17.4%.

The fourth row represents the results of the thermal analysis in a tropical climate. On the basis of weather data, the annual cooling degree-days represent 100% of the total degree-days (Table 1), which agrees with the results obtained from the thermal analysis. Also, the recommended model (sides) is also the best option based on results from the thermal analysis. The differences in total energy consumption were 6% compared with the central configuration, 5% compared with the half sides configuration, and 3.3% compared with the edge configuration.

Structural Performance Analysis

Because the objective of this study (and Yeang's recommendations) is to combine environmental and structural performance of the building cores, it is assumed that the vertical core/walls are the only components of the building's lateral load-resisting system. Yeang does not refer to the impact of the arrangement of the vertical core/walls on the structural performance. There is asymmetry in the floor plan in two configurations, the edge and the half sides, and structural asymmetry is known to lead to problems in structural performance; for example, impaired structural performance of the John Hancock building in Boston related to excessive torsional deformation under wind loading delayed opening for about 5 years and increased the total cost of the building to about twice the initial cost (Campbell et al. 1988). In three models (sides, half sides, and edge), the wall orientation provides lateral resistance and stiffness in only one direction; the orthogonal direction appears deficient to resist lateral loads. Past knowledge on successful structural systems for tall

buildings leads us to believe that the proposed lateral systems will not be sufficient for skyscrapers. Therefore, it is clear that additional lateral force-resisting systems will be needed in these buildings. In other words, the structural systems examined purely from an energy consumption perspective are not realistic and will not be adequate for these tall buildings. This is investigated in the next section.

Building Stiffness

Considering only the vertical core/walls as the lateral load-resisting system, preliminary calculations are made to investigate structural properties such as lateral stiffness, torsional stiffness, and effects of wind load eccentricity. The structural walls act as cantilevers independent of each other except for the central model, where walls compose a square core. Furthermore, the lateral stiffness is assumed to be dominated by flexural deformations, and the contribution of shear deformations on the system is neglected given the height of the models. The bending stiffness of each independent structural component i of the lateral force-resisting system is proportional to the product of the elastic modulus E and the cross-sectional moment of inertia I_i of the shear wall. The stiffnesses are denoted by k_i . The total bending stiffness of the lateral force resisting system K_{core} is the sum of the n individual component stiffnesses (see Fig. 8 for the coordinate system considered) and is proportional to the sum of the products EI_i (Smith and Coull 1991)

$$K_{\text{core}} = \sum_{i=1}^n k_i \propto \sum_{i=1}^n EI_i \quad (1)$$

where E is assumed constant for all walls. For a uniform wind load acting on a cantilever, the lateral bending stiffness can be calculated as follows:

$$k = \frac{8EI}{h^4} \quad (2)$$

where h = height of the structural wall. The concept of torsional stiffness of thin rectangular sections, such as the sides, the half sides, and the edge models, is used here to calculate the torsional stiffness of the structural wall as

Model	$K_{core} (Kn.m^2)$		$k (Kn/m)$		$k_t (Kn/m)$	$T (Kn.m)$	$\tau (MPa)$	Floor Plan
	x-axis	y-axis	x-axis	y-axis				
Sides	2025E	0.456E	$\frac{16200E}{h^4}$	$\frac{3.65E}{h^4}$	$\frac{1.82G}{h}$	0	0	
Half Sides	465E	0.279E	$\frac{3722E}{h^4}$	$\frac{2.23E}{h^4}$	$\frac{1.12G}{h}$	$9.2P_w$	$4.6P_w$	
Edge	0.5E	10659E	$\frac{4E}{h^4}$	$\frac{85272E}{h^4}$	$\frac{2G}{h}$	$20.3P_w$	$3.7P_w$	
Central	129.7E	129.7E	$\frac{1037E}{h^4}$	$\frac{1037E}{h^4}$	$\frac{230G}{h} \frac{c}{h}$	0	0	

Fig. 8. Lateral stiffness and torsional susceptibility of different building models (note that P_w is the wind pressure acting on the building; the arrows in the floor plan diagrams indicate the direction in which it acts)

$$k_t = \frac{bt^3G}{3h} \quad (3)$$

where G = shear modulus, b = length of the wall, and t = wall thickness. A structural asymmetry in plan about the vertical axis of the building generates eccentricity of the lateral loads from the center of stiffness of the building, leading to twisting in addition to translation of each floor. Here, plan eccentricity represents the horizontal distance perpendicular to each of the principal axes of the buildings determined between the position of the wind force resultant and the center of rigidity of the structural walls (Fig. 9). The torsional stiffness in the case of a square closed cross section, such as the core in the central model, can be calculated as follows (Ugural and Fenster 2003):

$$k_t = \frac{ta^3G}{h} \quad (4)$$

where a = side length of the square core. The location of the center of rigidity from an arbitrary origin is found using the following relationships:

$$\bar{x} = \frac{\sum_{i=1}^n k_{xi}x_i}{\sum_{i=1}^n k_{xi}} \quad (5)$$

$$\bar{y} = \frac{\sum_{i=1}^n k_{yi}y_i}{\sum_{i=1}^n k_{yi}} \quad (6)$$

where k_{xi} and k_{yi} = bending stiffnesses of the structural components about the x - and y -axes, respectively (see Fig. 8 for coordinate system).

The existence of floor eccentricity causes uniform wind pressure to generate torsional moments on the building. The resulting the torsional stress in the sides, the half sides, and the edge models is calculated as follows:

$$\tau = \frac{3T}{bt^2} \quad (7)$$

In the case of the central model (square core), the torsional stress is calculated as follows:

$$\tau = \frac{T}{2ta^2} \quad (8)$$

where T = twisting moment per unit height acting about a vertical axis of the building. This twisting moment results from the eccentricity (e), which is assumed to be the perpendicular distance between the center of pressure of the wind load P_w and the center of rigidity (CR) of the shear walls in floor plan

$$T = e \times P_w \quad (9)$$

Structural Performance Results

Fig. 8 summarizes the results of lateral stiffness calculations of the four models. The highest bending stiffness about the wall local x -axis was found in the sides model, the half sides model was second, the central model was third, and the edge model was fourth. Conversely, the highest bending stiffness about the wall local y -axis occurred in the edge model, whereas the half sides and the sides

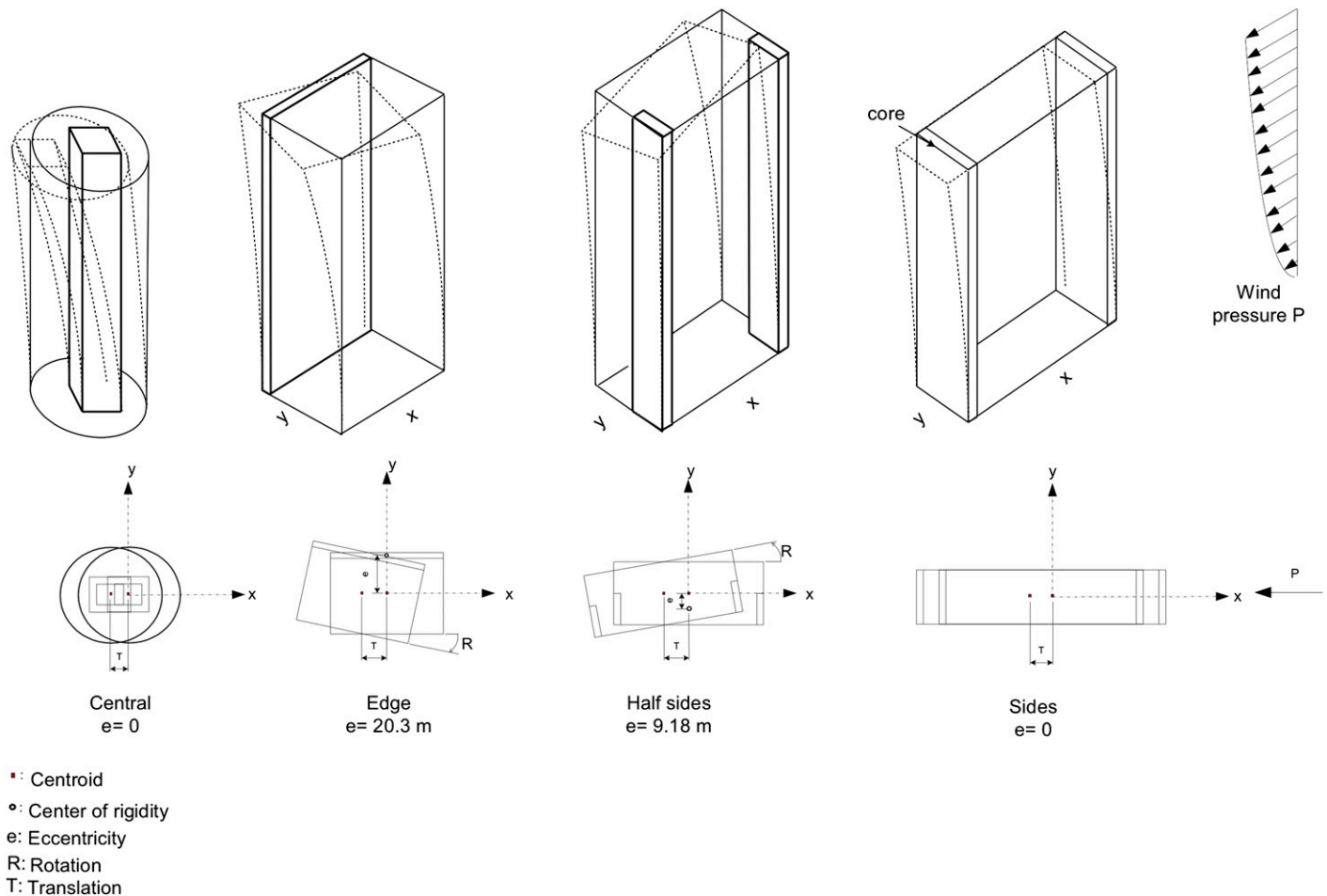


Fig. 9. Schematic deformations of different building types under wind loads

models were very flexible about the y -axis, and the central model maintained the same stiffness as before because of plan symmetry. Because lateral stiffness is directly related to area moment of inertia, the same behavior as observed in cross-sectional bending stiffness may be expected in building lateral stiffness.

The asymmetry in plan about the vertical axis of the building creates eccentricity that leads to two coupled displacement modes occurring under lateral loading (translation and rotation). This eccentricity is pronounced in two models: the edge and half sides models. Higher eccentricity leads to higher twisting moment and requires higher torsional stiffness. However, in the sides and central models, the only required torsional stiffness may be to meet minimum code-prescribed requirements or to account for winds coming from an angle. Moreover, in the case of the edge and half sides models, the design may be substantially affected by torsional stresses, with torsional stress in the half sides and edge models equal to $3.7P_w$ and $4.6P_w$, respectively. Fig. 9 shows 3D renderings that illustrate the different deformations that building types might exhibit under wind loads, where one mode of displacement (translation) occurs in the sides and central models, whereas two modes of displacement occur simultaneously in the half sides and edge models. A uniform wind load is assumed in this study. In an actual design, code provisions would prescribe a variable wind pressure, increasing with height. Use of such a wind profile would not qualitatively alter the results presented here, and therefore, a simple uniform wind profile is adopted. It is clear that the form of the building and the distribution of the

structural cores/walls would certainly substantially affect the stiffness and durability of the building.

Conclusions

In the context of optimizing the structural system of a building to improve energy efficiency in addition to resisting gravity and lateral loads, this paper examined four different building configurations for their ability to lower the energy consumption of skyscrapers. The results obtained from the thermal analysis shows, as in a previous study conducted by Yeang (1999), that the built-form configuration (foot-print shape and the placement of structural vertical core/wall) in the skyscraper's perimeter has significant effects on energy performance.

Also, the results show that in the four major climate zones, the placement of the structural vertical core/wall in the east and west sides and with an aspect ratio of 1:3, may lead to a reduction in energy consumption of 6–32% over the worst case design, depending on the climatic zone.

Asymmetric distribution of the structural walls, which occurs in some of the proposed building morphologies, may result in high torsional stresses and deformations caused by eccentricity between the center of wind pressure and the center of stiffness. To mitigate these stresses and deformations, supplemental structural systems have to be deployed in the building, increasing the cost and embodied energy of the structure. To consider this increase in embodied

energy alongside the operational energy expenditures that have been the focus of this paper, a full life-cycle cost analysis would be appropriate. Without extending the scope of this paper to such an analysis, such increased embodied energy must be considered in concert with the operational energy when attempting to design for environmental performance.

Last, Yeang (1999) suggests different wall distributions for sides, half sides, and edge configurations; these three configurations only provide stiffness and strength in one direction but are inadequate in the orthogonal direction of the building. It is clear then that structural configuration cannot be optimized or energy performance without significant implications for the structural performance.

The energy intensity calculations presented here demonstrate that there is substantial opportunity for architects and mechanical and structural engineers to collaborate on the selection of structural systems to improve sustainability. Preliminary structural calculations presented here, however, show that great care must be taken to ensure that optimization of the structural system for environmental performance does not compromise the ability of the system to resist structural loads and ensure safety and serviceability of the building.

Acknowledgments

The authors thank Carl Fiocchi for assistance in developing the Ecotect models. The Libyan Ministry of Education provided financial for this project. The University of Massachusetts, Amherst, also provided financial support.

References

- American Society of Heating, Refrigerating and 544 Air-Conditioning Engineers (ASHRAE). (2010). *Energy standard for buildings except low-rise residential buildings*, American Society of Heating, Refrigerating and Air-Conditioning Engineers, Atlanta.
- Anderson, J. E., and Silman, R. (2009). "The role of the structural engineer in green building." *Struct. Eng.*, 87(3), 28–31.
- Autodesk Education Community. (2011). (<http://students.autodesk.com/?nd=home>) (Sep. 1, 2010).
- Campbell, R., LeMessurier, W., Mahler, V. (1988). "Learning from the Hancock, 2 accounts of the failures and averted failures involving the famed Boston tower + interviews with LeMessurier, William and Mahler, Victor." *Architecture: AIA J.*, 77(3), 68–75.
- Chartered Institution of Building Services Engineers (CIBSE). (2006). "Environmental design." *CIBSE guide A*, Chartered Institution of Building Services Engineers, London.
- Chow, W. K. (2004). "Wind induced indoor airflow in a high rise building adjacent to a vertical wall." *Appl. Energy*, 77(2), 225–234, 10.1016/S0306-2619(03)00121-1.
- Jones, W., et al. (1982). *Passive solar design handbook, Vol. 3: Passive solar design analysis*, U.S. Department of Energy, Washington, DC.
- Kestner, D. M., Goupil, J., and Lorenz, E. (2010). *Sustainability guidelines for the structural engineer*, ASCE, Reston, VA.
- Kottek, M., et al. (2006). "World map of the Koppen-Geiger climate classification updated." *Meteorologische Zeitschrift*, 15(3), 259–263.
- Krem, M. A. M. (2012). "Effect of building morphology on energy and structural performance of high-rise office buildings." Ph.D. dissertation, Univ. of Massachusetts, Amherst, MA.
- Li, L., and Mak, C. M. (2007). "The assessment of the performance of a wind catcher system using computational fluid dynamics." *Build. Environ.*, 42(3), 1135–1141.
- Mak, C. M., Niu, J. L., Lee, C. T., and Chan, K. F. (2007). "A numerical simulation of wing walls using computational fluid dynamics." *Energy Build.*, 39(9), 995–1002.
- Mazria, E. (1979). *Passive solar energy book*, Rodale Press, Emmaus, PA.
- Smith, S., and Coull, A. (1991). *Tall building structures: Analysis and design*, Wiley, New York.
- Straube, J. (2006). "Green building and sustainability." *Building science digest*, U.S. Green Building Council, Green Building Research, Washington, DC.
- Ugural, C. A., and Fenster, S. K. (2003). *Advanced strength and applied elasticity*, Prentice Hall, Upper Saddle River, NJ.
- U.S. Department of Energy. (2010). "Energy efficiency and renewable energy." (http://apps1.eere.energy.gov/buildings/energyplus/cfm/weather_data.cfm) (Sep. 1, 2010).
- U.S. Department of Energy Building Energy Codes Program. (2010). *International energy conservation code*, International Code Council, Club Hills, IL.
- Webster, M. D. (2004). "Relevance of structural engineers to sustainable design of buildings." *Struct. Eng. Int.*, 14(3), 181–185, 10.2749/101686604777963874.
- Yeang, K. (1999). *The green skyscraper*, Prestel, New York.